Electronic Supplementary Information

Co-Tris coordination complex as a stable homogeneous electrocatalyst for aqueous water oxidation

Debu Jana, Kalipada Paul, and Samar K Das*

School of Chemistry, University of Hyderabad, P.O. Central University, Hyderabad – 500046, India

Email: skdas@uohyd.ac.in

Table of Contents:

Section S1. Experimental Section

Materials.

The chemicals, cobalt chloride ($CoCl_2 \cdot 6H_2O$, SRL, extra-pure AR, 99%), tris(hydroxymethyl)aminomethane ($C_4H_{11}NO_3$, SIGMA Life Science, 99%), sodium acetate (CH_3COONa, SIGMA ALDRICH, 99%) and distilled water are used for the preparation of compound $[Co\{NH_2C(CH_2OH)_2CH_2O\}\{NH_2C(CH_2OH)_3\}(CH_3COO)(H_2O)]$ (**CoT**). For electrochemistry, Milli-Q water has been used. The electrodes, glassy carbon, fluorine-doped tin oxide (FTO), platinum wire, and Ag/AgCl (3M KCl) were purchased from Sinsil Int. Pvt. Limited (India).

Preparation of CoT complex.

Initially, a 0.1 M sodium acetate buffer solution of pH 7.2 was prepared by dissolving the required amount of NaOAc in Milli-Q water. Then, $CoCl_2.6H_2O$ (11.9 mg, 0.05 mmol) was dissolved in 10 mL of 0.1 M sodium acetate solution. After getting a clear pink solution, the Tris base ligand (tris(hydroxymethyl)aminomethane) (30.3 mg, 0.25 mmol) was dissolved. The resulting solution was allowed to be shaken by hand for 30 minutes. After 30 minutes, a deep-green-colored solution was obtained. In this study, the obtained solution has been defined as a **CoT** complex for homogeneous electrocatalytic water oxidation.

Characterization methods.

We have recorded IR data using an iD7 ATR Thermo Fisher Scientific-Nicolet iS5 instrument. The Raman data were collected from the HORIBA He-Ne Laser 532 nm Micro-Raman spectroscopy instrument. The DRS-UV-visible spectral data were collected from the SHIMADZU UV-2600 instrument. We have recorded the PXRD data from the Panalytical X'pert powder diffractometer equipped with a Cu-K_α source (λ = 1.540598 Å) instrument. The XPS data were carried out using the X-ray Photo Spectrometer and UPS Model- K ALPHA + Make- M/s Thermo Fisher Scientific Instruments UK, Vacuum details. The Carl Zeiss model Ultra 55 microscope was used for field emission scanning electron microscope (FESEM) imaging and energy dispersive X-ray (EDX) analysis. Solution UV-visible studies were carried out using a JASCO V-750 spectrophotometer. ^1H and ^{13}C NMR analyses were performed using the 500 MHz and 125 MHz Advance Bruker spectrometers, respectively. Chemical shifts (δ) are reported in ppm. The HRMS data were collected from the Bruker-Maxis, ESI-QTOF instrument.

Electrochemical OER measurements.

In this study, we have used a three-electrode cell consisting of a working electrode (glassy carbon: 3 mm diameter / FTO: 0.5 cm × 0.5 cm surface area), counter electrode (platinum wire) and reference electrode (Ag/AgCl, 3 M KCl). The 0.1 M NaOAc electrolyte was initially prepared in a neutral pH (7.2). After adding $CoCl_2 \cdot 6H_2O$ and Tris base, the pH of the resultant solution was measured to be 8.5 and placed into the electrochemical cell with three electrodes for OER studies. All electrochemical experiments were performed on a Princeton Applied Research Instrument (PARSTAT) operated with Versastudio software. Electrode potentials were converted to the NHE scale using the relation E(NHE) = E(Ag/AgCl) + 0.197 V, where Ag/AgCl (3M KCl) electrode was used as a standard electrode.

==========

Section S2. Density functional theory (DFT) study of CoT[1]

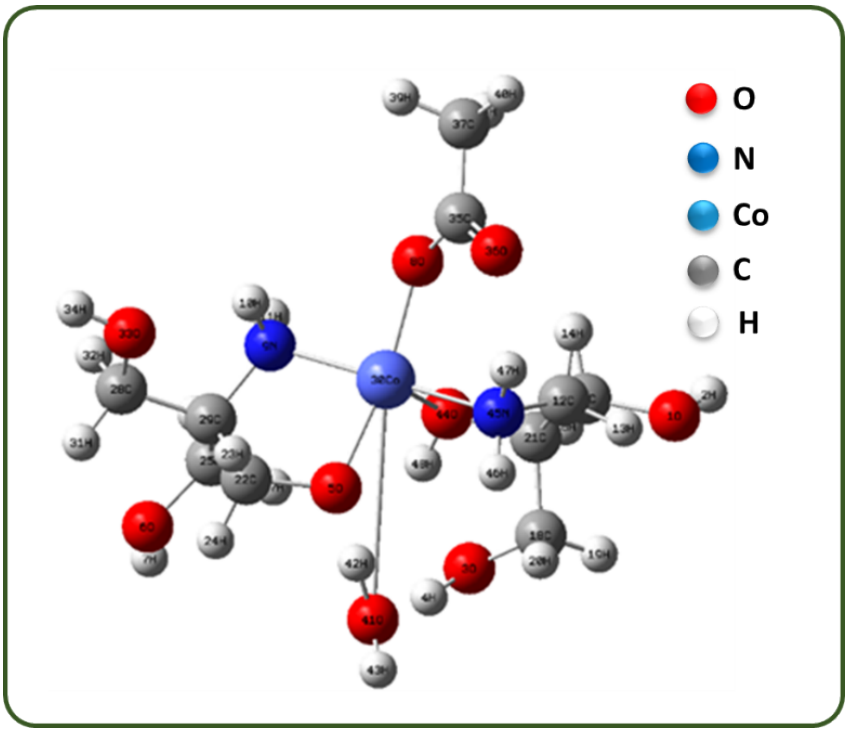

Fig. S1 Optimized ground state geometry for **CoT** complex calculated at the B3LYP/LANL2DZ level of theory.[1]

Table S1. Optimized coordinates of CoT complex[1]

O	4.80332462	-1.15765059	-0.83830599
H	5.49613916	-1.19707408	-1.52925070
O	1.33732172	-3.22706122	-0.23401755
H	0.54760689	-3.31921881	0.43743759
O	-1.11974811	-0.72734793	1.30362980
O	-3.74439517	-2.30611550	-0.95998511
H	-3.62409421	-3.14514154	-1.45031056
O	0.59246180	2.23615802	-0.54271128
N	-1.78046691	0.86805110	-0.72877508
H	-2.13844525	1.80192792	-0.49165208
H	-1.56643478	0.86005993	-1.73064495
C	2.70929625	0.12586173	0.68155376
H	3.55951463	-0.13744230	1.32170618
H	2.97194770	1.03241361	0.12926770
C	3.47785726	-1.01698260	-1.44978689
H	3.27643027	-1.85371448	-2.13419809
H	3.40521131	-0.07213329	-2.00554109
C	2.37776846	-2.41950256	0.39090931
H	3.34483883	-2.91942283	0.28367861
H	2.15988918	-2.30391208	1.46116950
C	2.44297408	-1.01988322	-0.31306324
C	-2.54691906	-0.50694897	1.12832122
H	-2.88571947	0.31672630	1.77177859
H	-3.10033358	-1.41493457	1.40152191
C	-2.64894669	-1.38290606	-1.25872522
H	-2.68782061	-1.08277409	-2.31719930
H	-1.68037487	-1.85471253	-1.05184965
C	-4.23786923	0.44584562	-0.54162367
C	-2.82930782	-0.15179807	-0.35248765
Co	-0.11047171	0.61877136	0.33204164
H	-4.98705954	-0.19641685	-0.06578229
H	-4.47173465	0.53928691	-1.61176672
O	-4.21810781	1.77398097	0.08792240
H	-5.07289784	2.23268106	-0.04148900
C	1.16900159	3.25830394	0.06006036
O	1.51622348	3.26402025	1.29493785
C	1.40754220	4.48067664	-0.81853654
H	1.94113997	4.18953927	-1.73064056
H	0.44427946	4.90881832	-1.12348274
H	1.98336312	5.23778768	-0.28033663
O	-0.55257706	-3.10953716	1.40019114
H	-0.81562493	-2.05630456	1.41782701
H	-0.63705488	-3.56936285	2.25392601
O	1.12887651	-0.77876993	-0.94193114
N	1.49308696	0.44702314	1.49370104
H	1.32050652	-0.23299036	2.23691651
H	1.58204335	1.40308196	1.87505997
H	0.75365786	-1.69652830	-1.06332113

==========

Section S3. Homogeneous electrocatalytic water oxidation.

Section S3.1. Electrochemical experiments for OER activity and stability check of CoT complex.

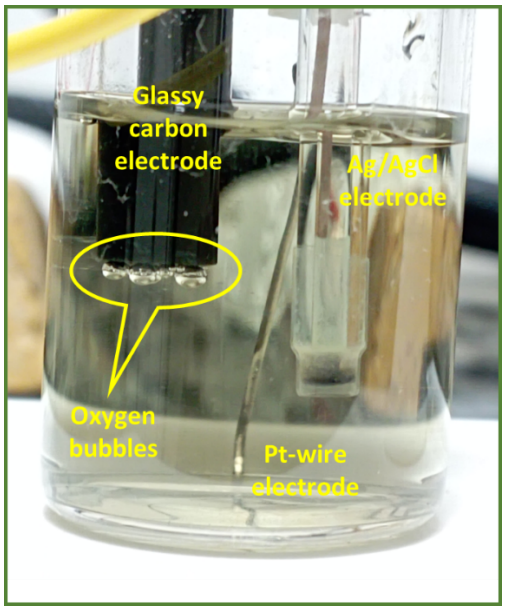

Fig. S2 Oxygen gas bubbles on the surface of the glassy carbon working electrode during the constant potential electrolysis (CPE) of homogeneous solution of **CoT** complex at a constant potential of 1.40 V (vs. NHE) for 2 h.

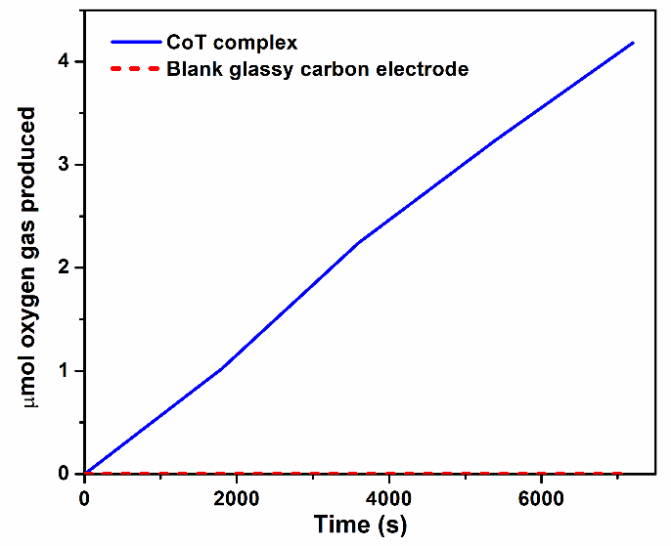

Fig. S3 Oxygen gas produced *versus* time plot of **CoT** complex (blue line) and blank glassy carbon electrode (red line), observed from the home-made electrochemical cell during the constant potential electrolysis at 1.40 V (vs. NHE) for 2 h.

Section S3.1.1. Quantitative analysis of the oxygen gas during bulk electrolysis:

We have carried out bulk electrolysis (constant potential electrolysis) of **CoT** complex at a constant potential of 1.5 V (*vs.* NHE) for a period of 2 h with the help of a home-built three-electrode electrolysis setup, as shown in Fig. S4, below.[2] This set-up contains a glassy carbon (GC) electrode (diameter: 3 mm) as the working electrode, a Pt-wire as the counter electrode, and an Ag/AgCl electrode as the reference electrode.

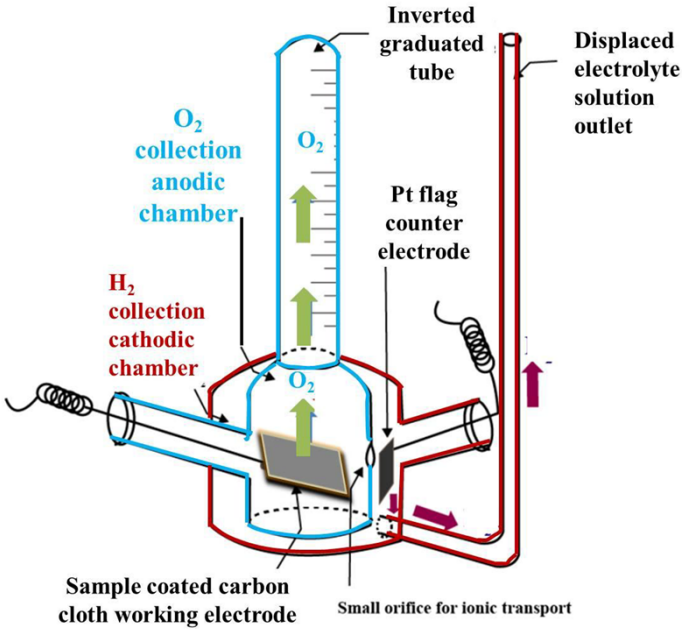

Fig. S4 Schematic representation of the home-made quantitative gas determination setup used to calculate the Faradic efficiency.[2-3]

The oxygen gas (product gas bubbles) was identified as only oxygen gas using a gas chromatography study (Fig. 1d, main text). The oxygen gas evolved at the surface of the GC electrode during the electrolysis of **CoT** complex was gradually collected in a graduated tube of the home-built electrolysis setup, and slowly, the solution in the graduated tube was displaced by these oxygen gas bubbles. The hydrogen gas that was evolved at the counter electrode could not mix with the oxygen gas evolved at the working electrode, because the setup was built in such a way that the gas evolved in the anodic chamber could not enter the cathodic chamber. The two chambers were separated from each other by an inverted glass tube, and a small window was kept open between them to maintain the electrical continuity (Fig. S4, shown above).

Calculation of Faradaic efficiency:

In this bulk electrolysis experiment, the amount of the evolved oxygen gas for 2 h is 0.1 mL under 1 atm pressure at 25 °C (Fig. S5, shown below).

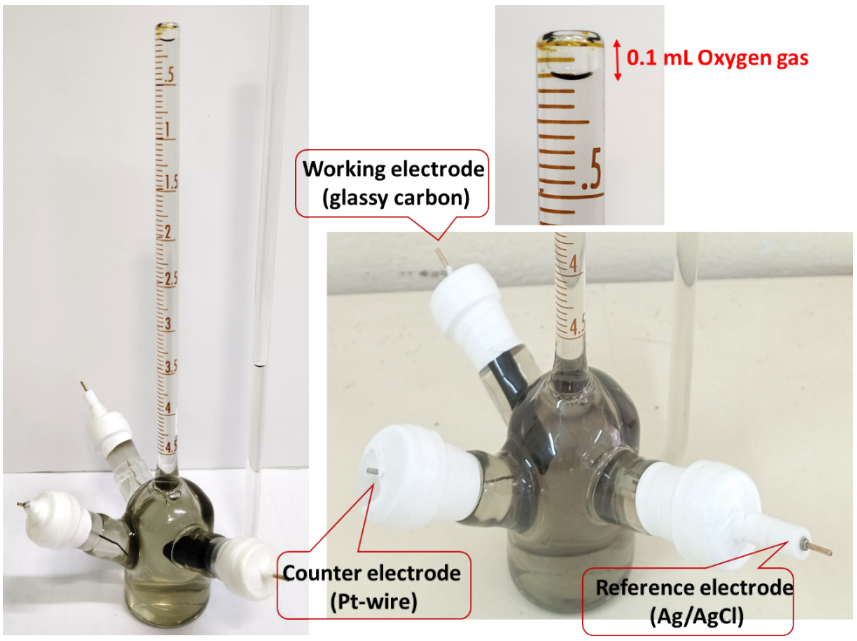

Fig. S5 Real image of the home-made quantitative gas determination setup used to calculate the Faradaic efficiency of **CoT** complex for water oxidation.

Therefore, the number of moles of O_2 gas found in 2 h = (0.1/24500) = **4.0816×10^{-6} mole**

(Note: At 1 atm pressure at 25 °C, 1 mole = 24500 mL)

Now, the number of moles of O_2 gas, evolved ideally, is expressed in equation S1 (shown below),

$$\mathbf{O_2\ (ideal)} = \frac{Q\ (total\ charge\ employed)}{n\ (number\ of\ electrons\ required\ for\ the\ chemical\ change) \times 1\ Farad} \quad \text{(S1)}$$

In this work, the **CoT** complex is involved in the $4e^-$ oxidation process, as shown in equation S2 (shown below).

$$O_2 + 4H^+ + 4e^- \rightarrow 2H_2O \quad \text{(S2)}$$

From the bulk electrolysis, we have calculated the total charge accumulated for oxygen gas production. From Fig. R6 (shown below), we have calculated the total charge (Q) as 1.67 C.

Here, O_2 (ideal) in 2 h = (1.67 C) / (4 × 96500 C·mol^{-1}) = **4.3264 × 10^{-6} mole**.

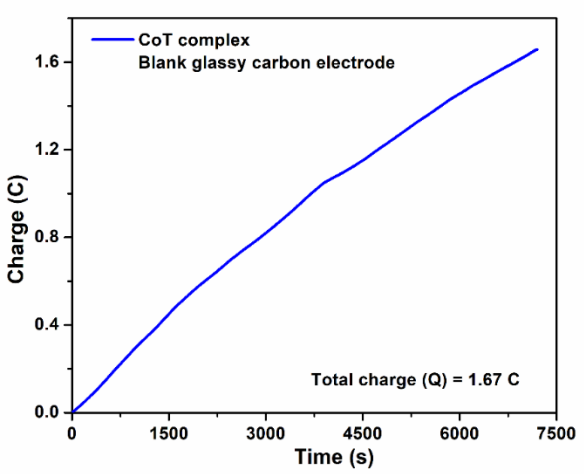

Fig. S6 Charge *versus* time plot of 5 mM **CoT** complex during the constant potential electrolysis for 2 h.

Now, the formula for Faradaic Efficiency is expressed in equation S3 (shown below),

$$\textbf{Faradaic efficiency} = \frac{Moles\ of\ oxygen\ evolved\ by\ experiment}{Moles\ of\ oxygen\ evolved\ by\ ideal} \times 100 \qquad \text{(S3)}$$

Finally, Faradaic Efficiency of compound **1** = [(4.0816 × 10^{-6}) / (4.3264 × 10^{-6})] × 100 = **94.34 %**

We have measured the error bar of ± 0.005 mL of oxygen gas after 2 h of electrolysis. Accordingly, the Faradaic efficiency is calculated to be **(94.3 ± 4.7) %**.

Turnover number (TON) and Turnover frequency (TOF):

In the bulk electrolysis, ~4 × 10^{-6} mmol of **CoT** complex generates 4.0816 × 10^{-6} mole of oxygen gas over 2 h. Thus, the turnover number (TON) of the **CoT** complex for the oxygen production is calculated as ~1.02 over 2 h. Therefore, the turnover frequency (TOF) of the **CoT** complex for the oxygen production is calculated as ~0.51 h^{-1}.

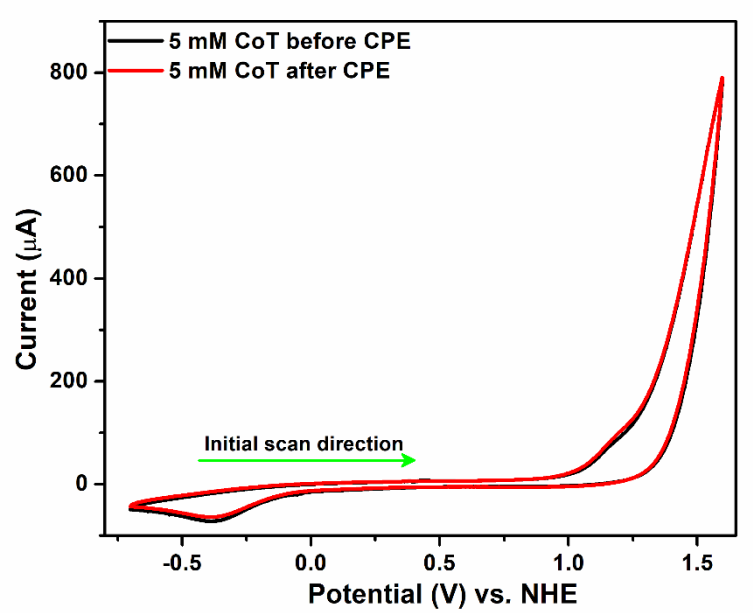

Fig. S7 CV diagrams of 5 mM **CoT** complex before (black line) and after (red line) the 2 h CPE experiment (working electrode: glassy carbon, reference electrode: Ag/AgCl, counter electrode: Pt wire, scan rate: 100 mV/s).

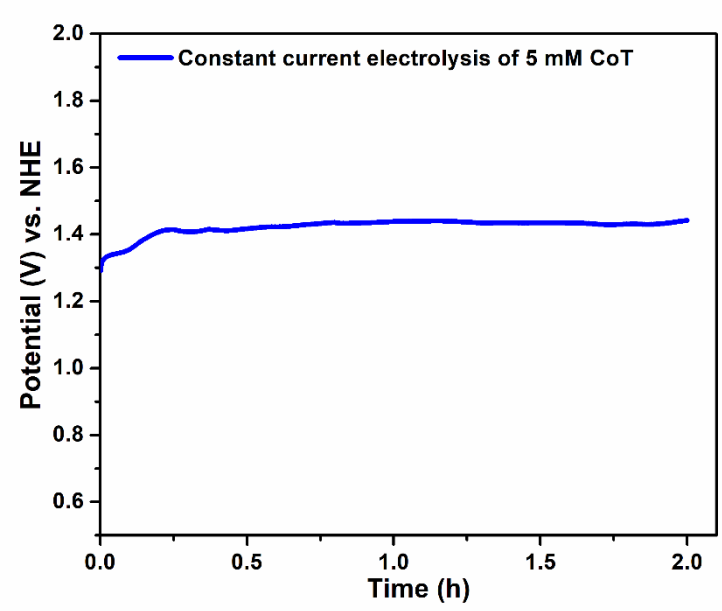

Fig. S8 Constant current electrolysis (CCE) of 5 mM **CoT** complex at a constant current of 70 μA for 2 h (working electrode: glassy carbon, reference electrode: Ag/AgCl, counter electrode: Pt wire).

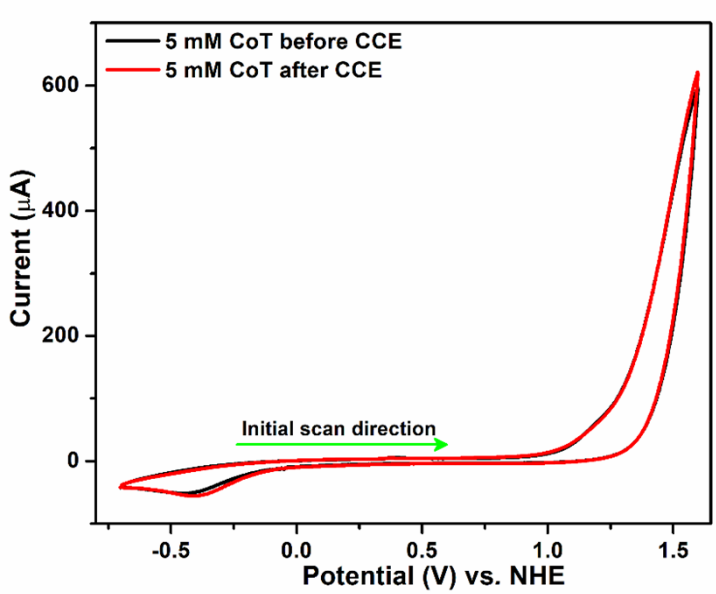

Fig. S9 CV diagrams of 5 mM **CoT** complex before (black line) and after (red line) the 2 h CCE experiment (working electrode: glassy carbon, reference electrode: Ag/AgCl, counter electrode: Pt wire, scan rate: 100 mV/s).

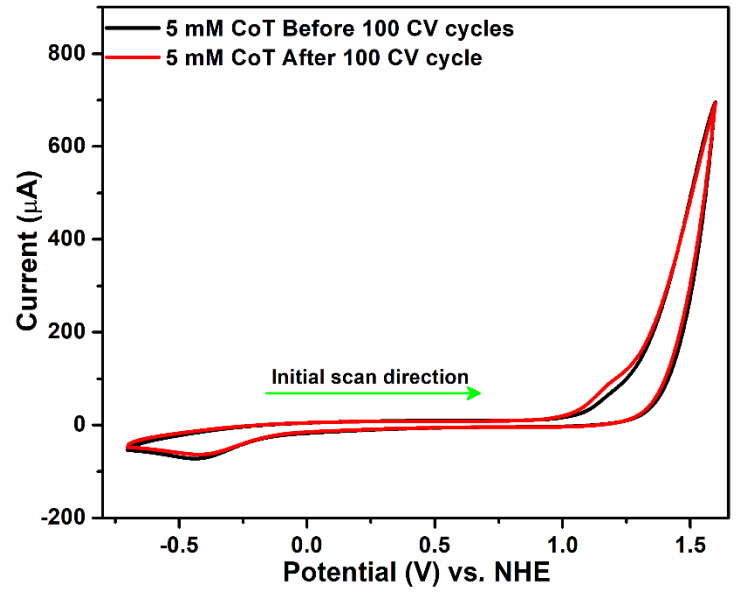

Fig. S10 CV diagrams of 5 mM **CoT** complex before (black line) and after (red line) multiple (100) CV cycling experiment (working electrode: glassy carbon, reference electrode: Ag/AgCl, counter electrode: Pt wire, scan rate: 100 mV/s).

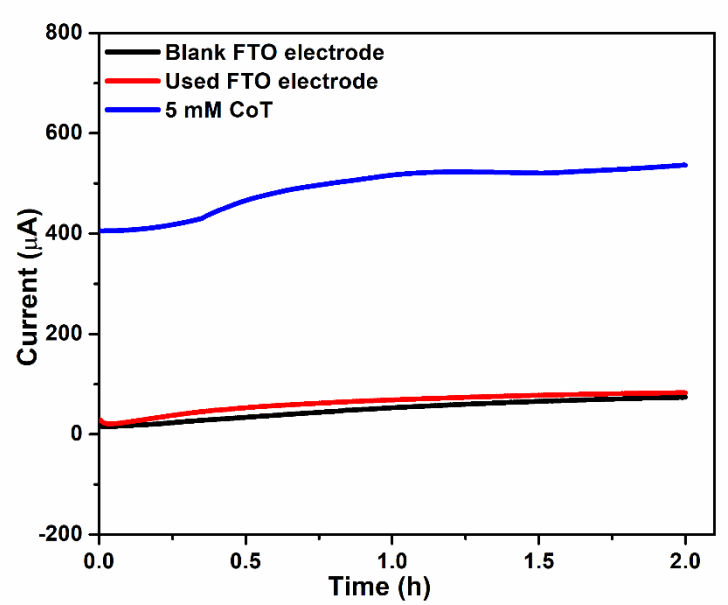

Fig. S11 Constant potential electrolysis (CPE) plots of 5 mM **CoT** complex (blue line) using FTO working electrode, used (in 2 h CPE) FTO electrode in fresh 0.1 M NaOAc aqueous electrolyte after 2 h CPE (red line) and blank FTO electrode in fresh 0.1 M NaOAc aqueous electrolyte (black line) at a constant potential of 1.40 V (vs. NHE) for 2 h (reference electrode: Ag/AgCl, counter electrode: Pt wire).

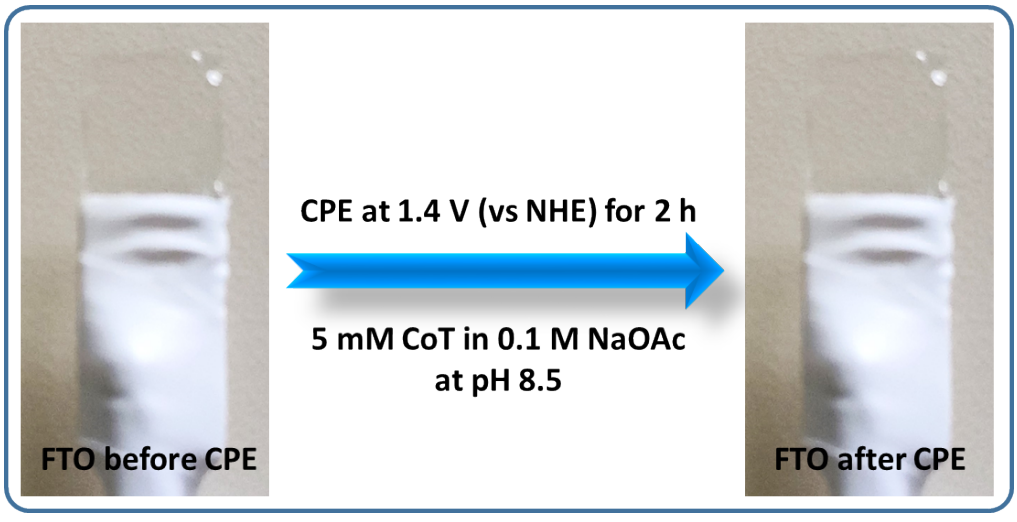

Fig. S12 Photographs of FTO working electrodes before and after the constant potential electrolysis (CPE) of 5 mM **CoT** complex in 0.1 M NaOAc aqueous electrolyte (pH 8.5) at a constant potential of 1.40 V (vs. NHE) for 2 h.

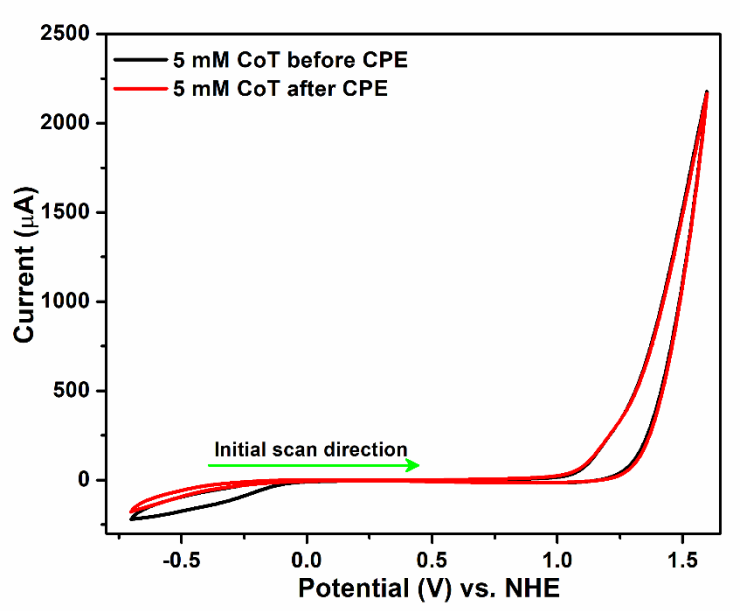

Fig. S13 CV diagrams of 5 mM **CoT** complex before (black line) and after (red line) the 2 h CPE experiment (working electrode: FTO, reference electrode: Ag/AgCl, counter electrode: Pt wire, scan rate: 100 mV/s).

==========

Section S3.2. Solution stability check of CoT complex during electrolysis.

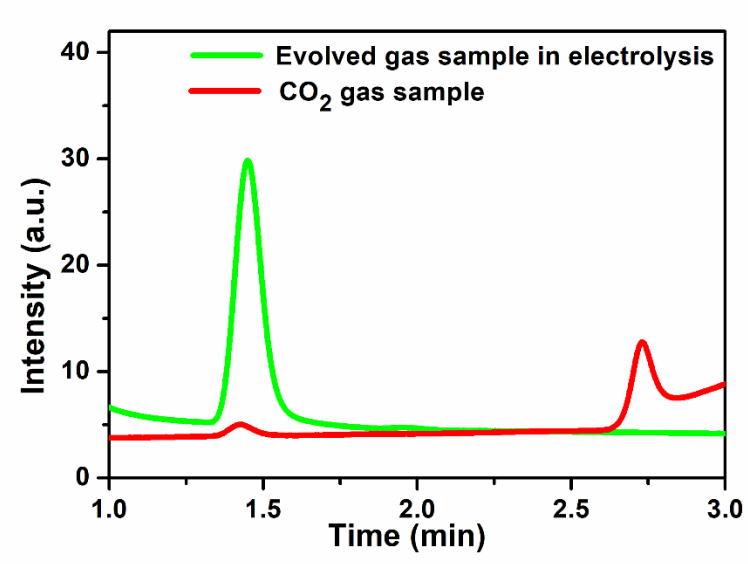

Fig. S14 Gas chromatography (GC) diagrams of the evolved gas sample during electrolysis, catalyzed by **CoT** complex (green line) and pure CO_2 gas sample (red line). The GC diagram of a pure CO_2 gas sample shows a tiny O2 peak because O2 enters from the air during the injection of the CO_2 gas sample.

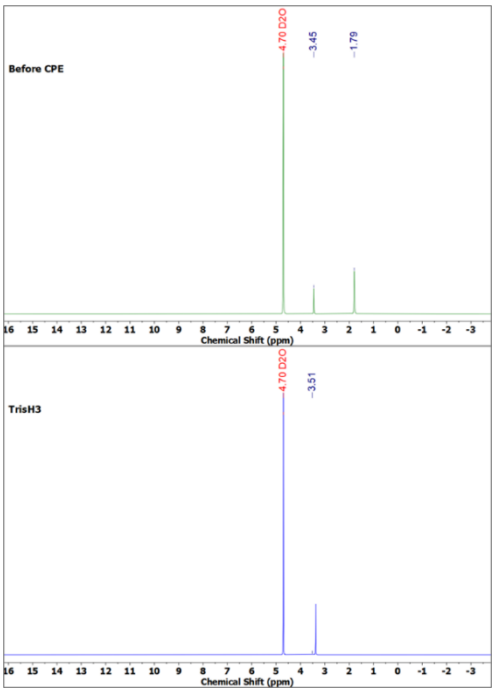

Fig. S15 ^{1}H NMR spectra of Tris base ligand in D_2O solvent (bottom) and **CoT** complex solution in D_2O solvent (top) using a 500 MHz NMR instrument.

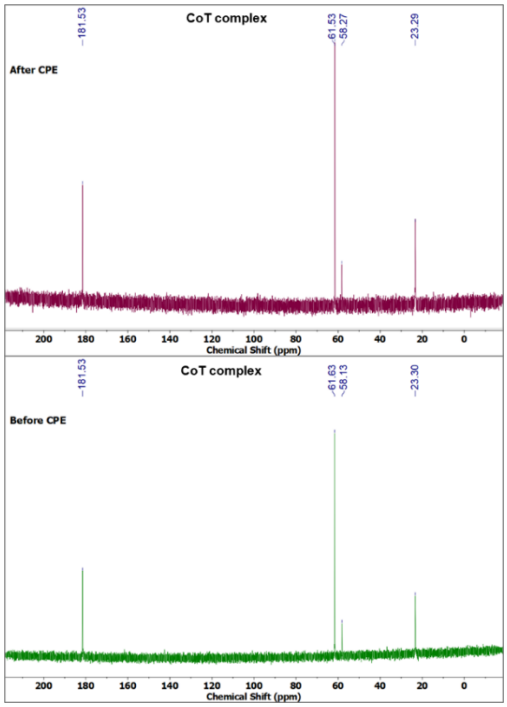

Fig. S16 ^{13}C NMR spectra of **CoT** complex solution in D_2O solvent, before (bottom) and after (top) the CPE analysis using a 125 MHz NMR instrument.

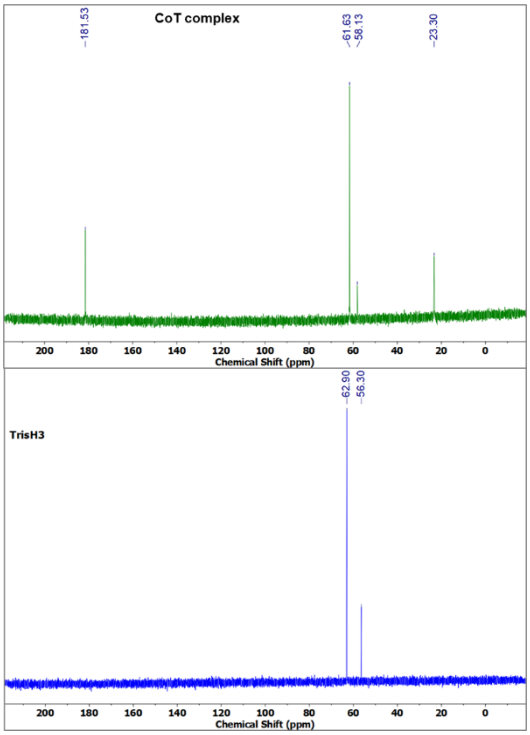

Fig. S17 ^{13}C NMR spectra of Tris base ligand in D_2O solvent (bottom) and **CoT** complex solution in D_2O solvent (top) using a 125 MHz NMR instrument.

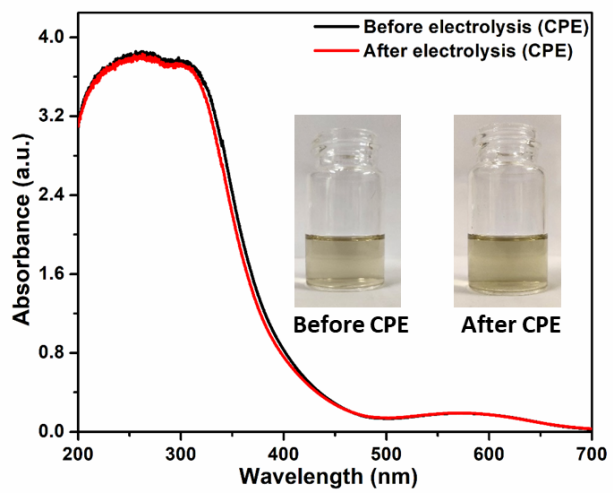

Fig. S18 UV-visible spectra of **CoT** complex solutions, before and after the CPE analysis.

==========

Section S3.3. Electrodeposition check of CoT complex during electrolysis.

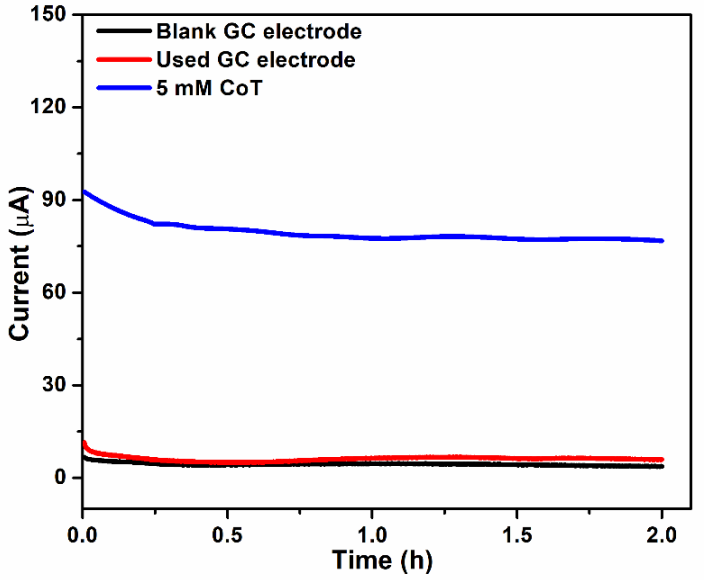

Fig. S19 Constant potential electrolysis (CPE) plots of **CoT** complex (blue line), used (in 2 h CPE) glassy carbon electrode in fresh 0.1 M NaOAc aqueous electrolyte after 2 h CPE (red line) and blank glassy carbon electrode in fresh 0.1 M NaOAc aqueous electrolyte (black line) at a constant potential of 1.40 V (vs. NHE) for 2 h (reference electrode: Ag/AgCl, counter electrode: Pt wire).

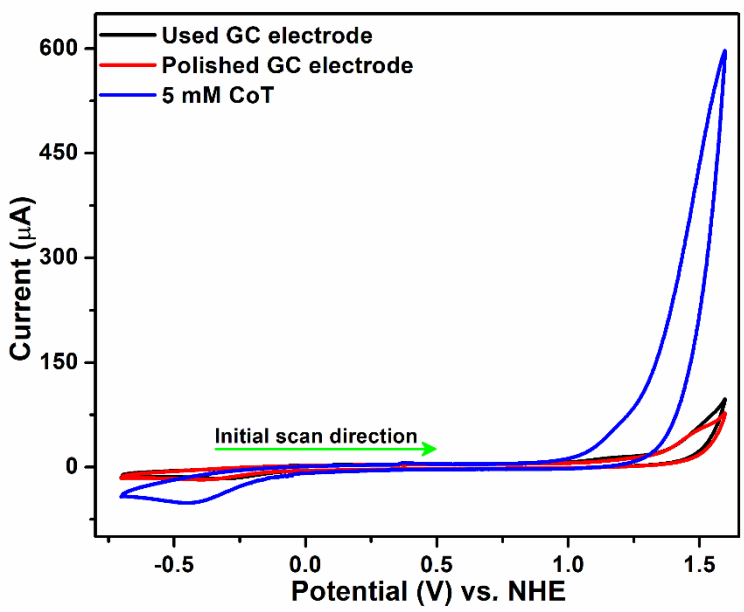

Fig. S20 CV diagrams of rinse test: 5 mM **CoT** complex (blue line), used (in CCE) glassy carbon electrode in fresh 0.1 M NaOAc aqueous electrolyte after 2 h CCE (black line) and polished glassy carbon electrode in fresh 0.1 M NaOAc aqueous electrolyte after 2 h CCE (red line) (reference electrode: Ag/AgCl, counter electrode: Pt wire, scan rate 100 mV/s).

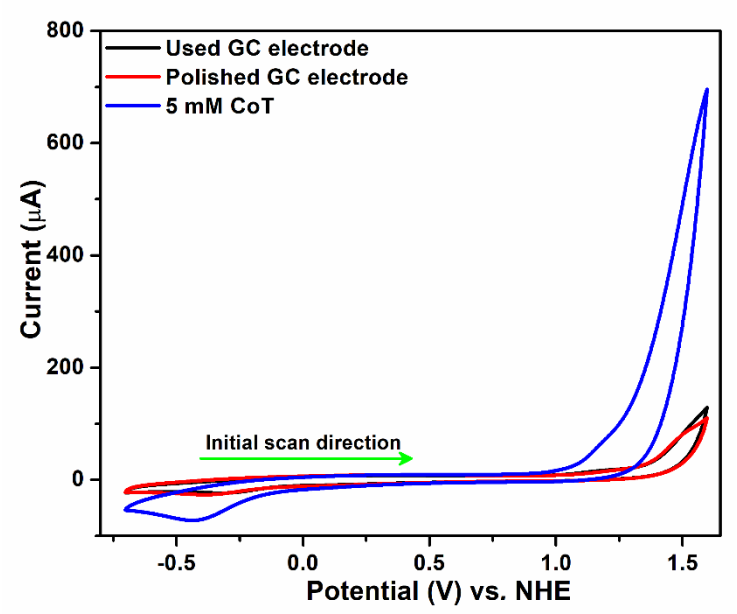

Fig. S21 CV diagrams of rinse test: 5 mM **CoT** complex (blue line), used (in 100 CV cycling) glassy carbon electrode in fresh 0.1 M NaOAc aqueous electrolyte after 100 CV cycling (black line) and polished glassy carbon electrode in fresh 0.1 M NaOAc aqueous electrolyte after 100 CV cycling (red line) (reference electrode: Ag/AgCl, counter electrode: Pt wire, scan rate 100 mV/s).

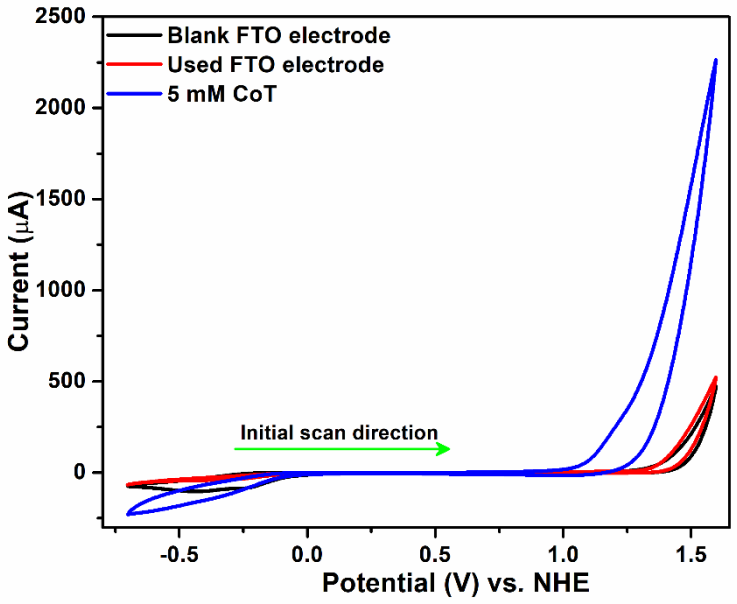

Fig. S22 CV diagrams of rinse test: 5 mM **CoT** complex (blue line), used (in CPE) FTO electrode in fresh 0.1 M NaOAc aqueous electrolyte after 2 h CPE (red line) and blank FTO electrode in fresh 0.1 M NaOAc aqueous electrolyte after 2 h CPE (black line) (reference electrode: Ag/AgCl, counter electrode: Pt wire, scan rate 100 mV/s).

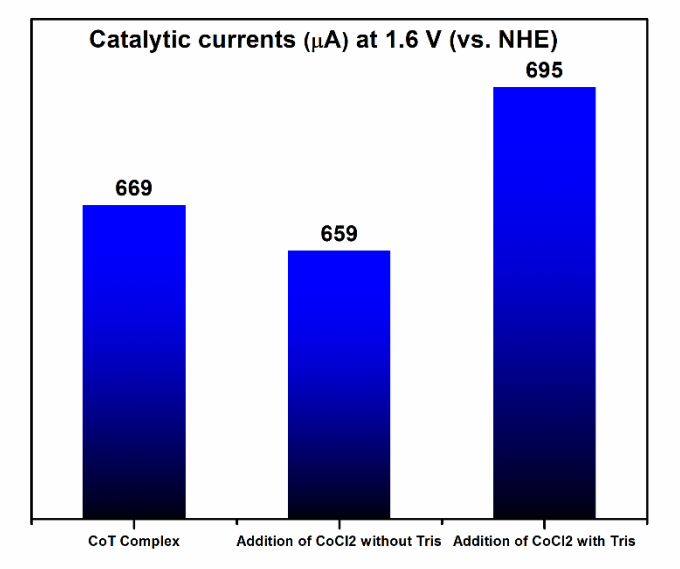

Fig. S23 Bar diagram of catalytic currents at 1.6 V (vs. NHE), obtained from Fig. 3b.

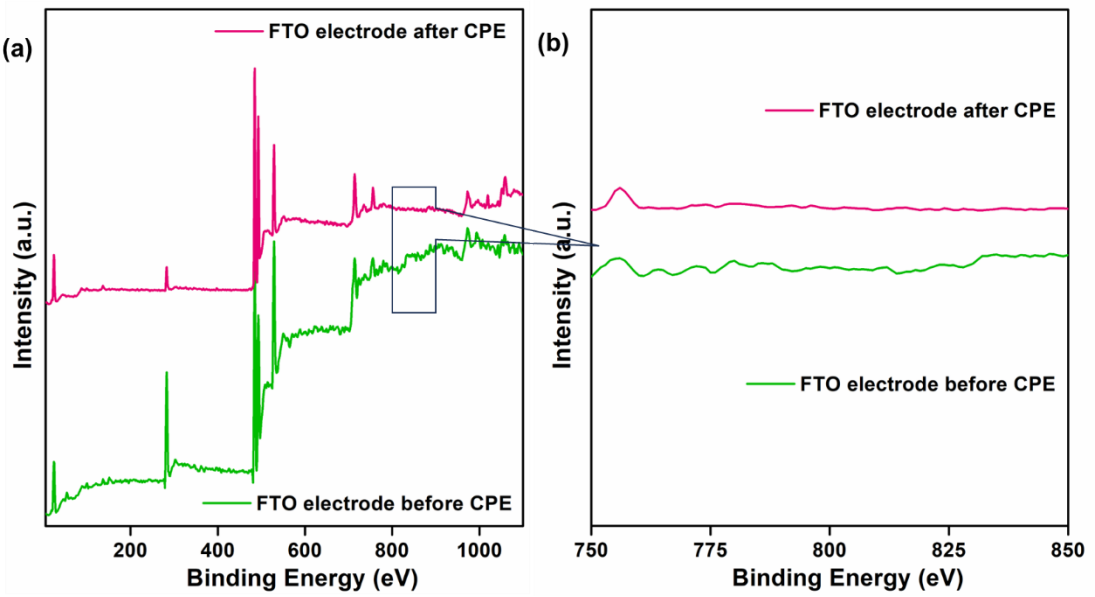

Fig. S24 XPS spectra of FTO working electrodes before and after the CPE analysis. (a) Full and (b) spectra show no CoO_x electrodeposition in this binding energy region.

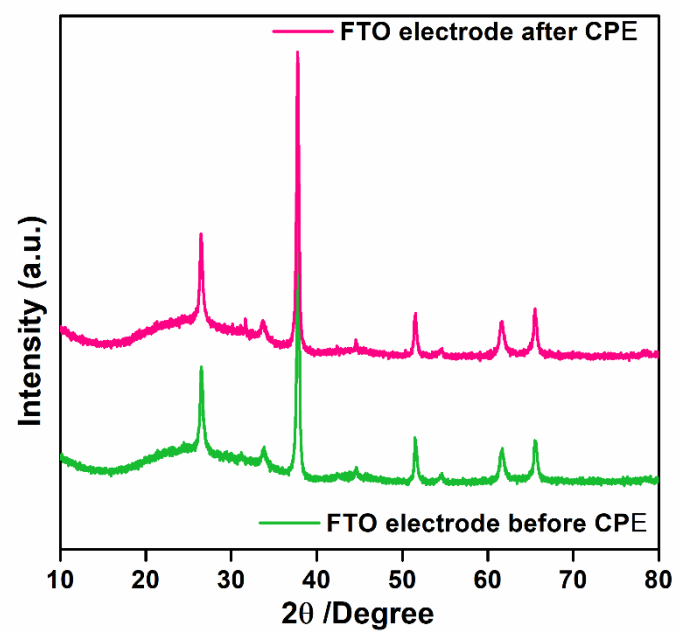

Fig. S25 PXRD patterns of FTO working electrodes before and after the CPE analysis.

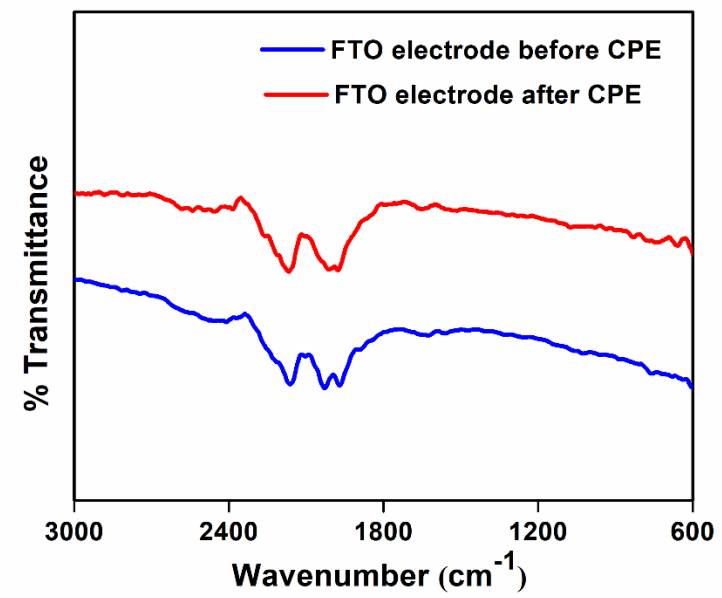

Fig. S26 IR plots of FTO working electrodes before and after the CPE analysis.

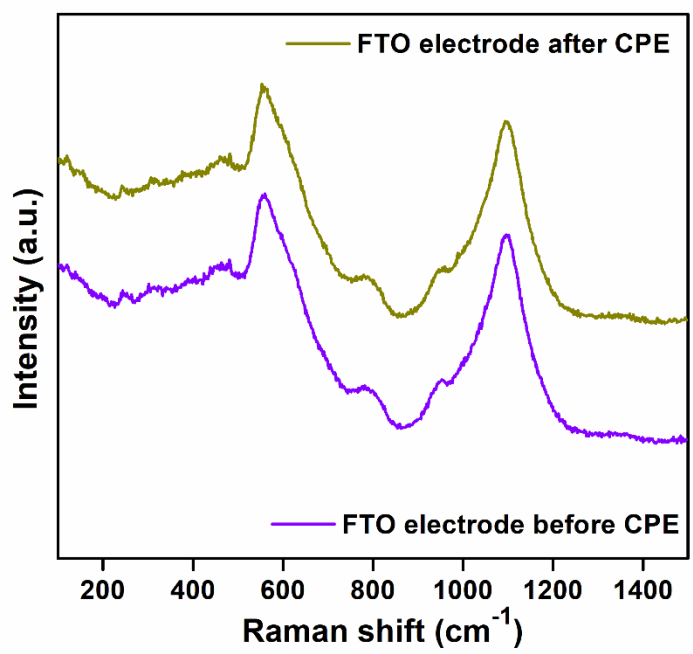

Fig. S27 Raman plots of FTO working electrodes before and after the CPE analysis.

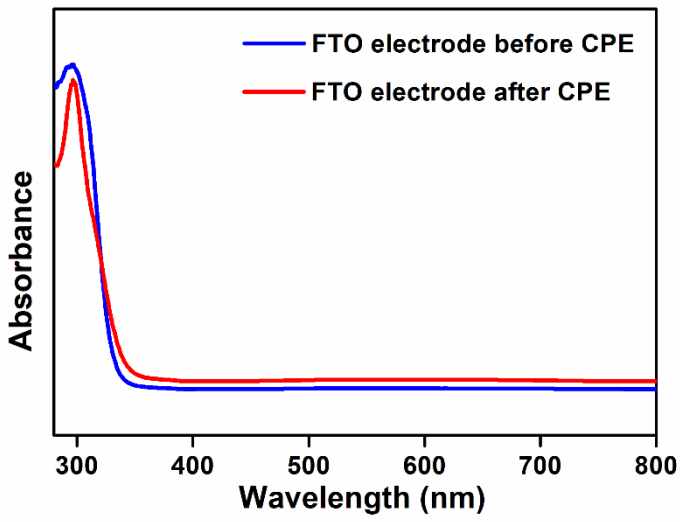

Fig. S28 UV-visible DRS plots of FTO working electrodes before and after the CPE analysis.

==========

Section S4. Experiments for kinetic insight.

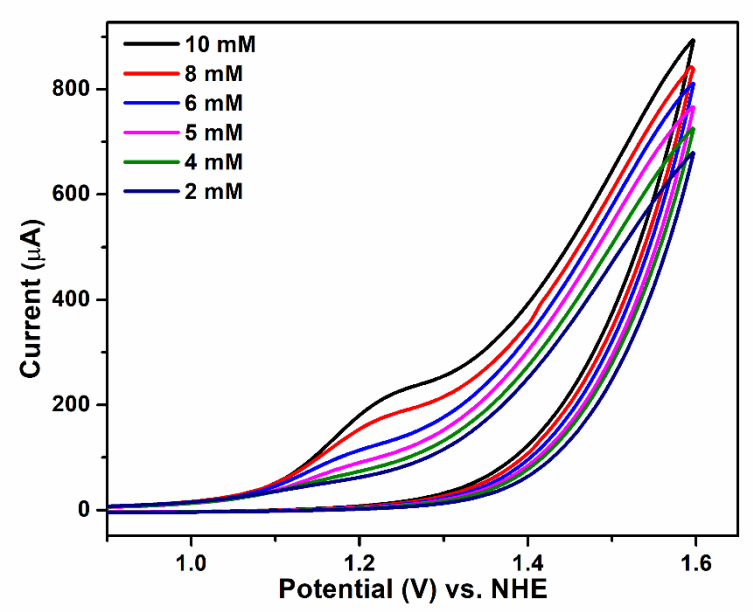

Fig. S29 CV diagrams of the catalyst (**CoT** complex) at various concentrations (working electrode: glassy carbon, reference electrode: Ag/AgCl, counter electrode: Pt wire, scan rate 100 mV/s).

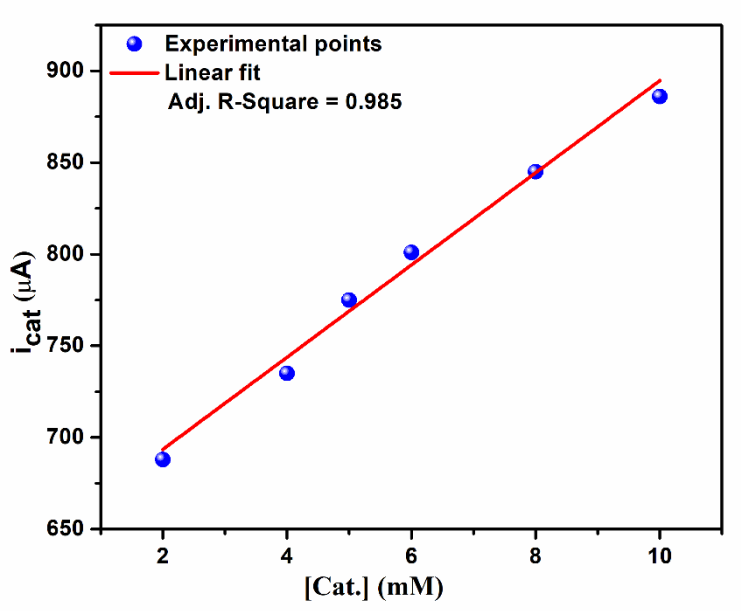

Fig. S30 Linear fitted plot of i_{cat} versus concentration of the catalyst (**CoT** complex) from Fig. S29.

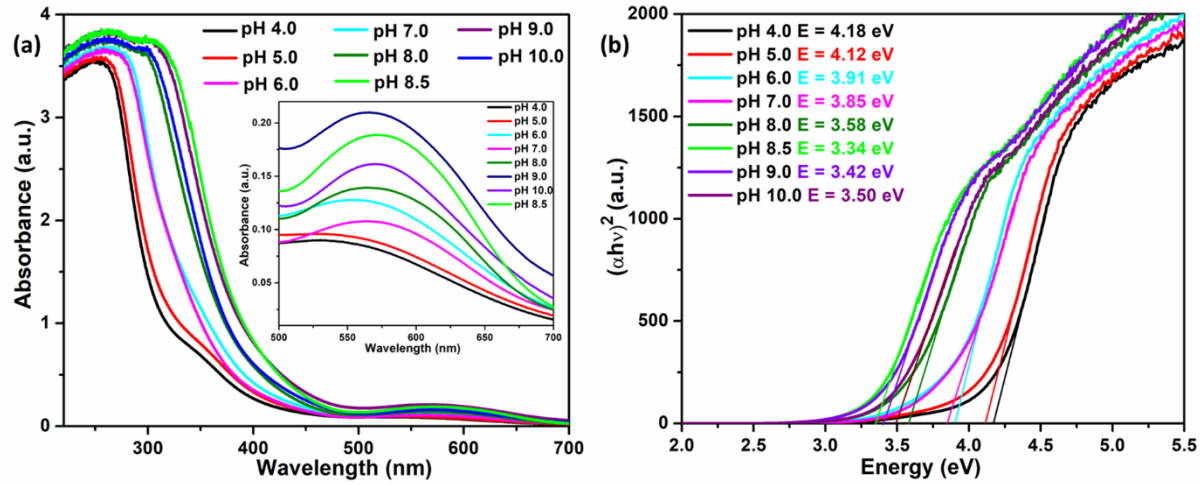

Fig. S31 (a) UV-visible spectra of catalyst (**CoT** complex) solutions at various pH values, inset image: spectra in visible region; (b) Tauc plots of catalyst (**CoT** complex) solutions at various pH values.

Section S4.1. Coulometry experiment.

In a Coulometry experiment, we performed a bulk electrolysis (constant potential electrolysis) at a constant potential of 1.40 V (vs. NHE) for 2 h using a three-electrode electrochemical cell containing 10 mL of 5 mM of **CoT** complex solution, FTO working electrode (1 × 1 cm^2), Pt-wire counter electrode, and Ag/AgCl reference electrode. From Fig. S32 (shown below), we have calculated the total charge consumed by the **CoT** complex over 2 h as 9.01 C. The number of electrons transferred during bulk electrolysis was calculated by Faraday's law of electrolysis $Q = nFN$, where Q is the number of coulombs (charge), F (Faraday's constant) is 96485 C/mol, N is the moles of substrate electrolyzed, and n is the stoichiometric number of electrons consumed. In this case, we have calculated the 'number of electrons consumed (n)' by the Co(II) center of **CoT** complex as 1.9 (≈2.0). Thus, in this bulk electrolysis at 1.40 V (vs. NHE), the Co(II) center is involved in two-electron oxidation to generate the Co(IV) center.

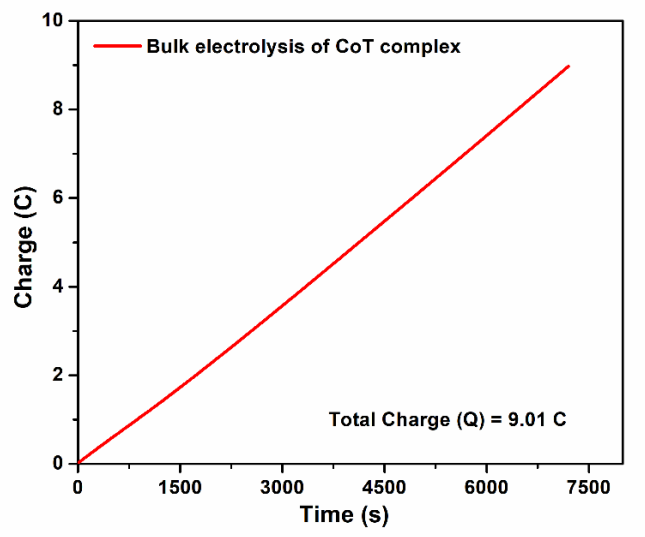

Fig. S32 Charge *versus* time plot of 5 mM **CoT** complex during the constant potential electrolysis at 1.40 V (vs. NHE) for 2 h, using FTO working electrode (1 × 1 cm^2), Pt-wire counter electrode, and Ag/AgCl reference electrode.

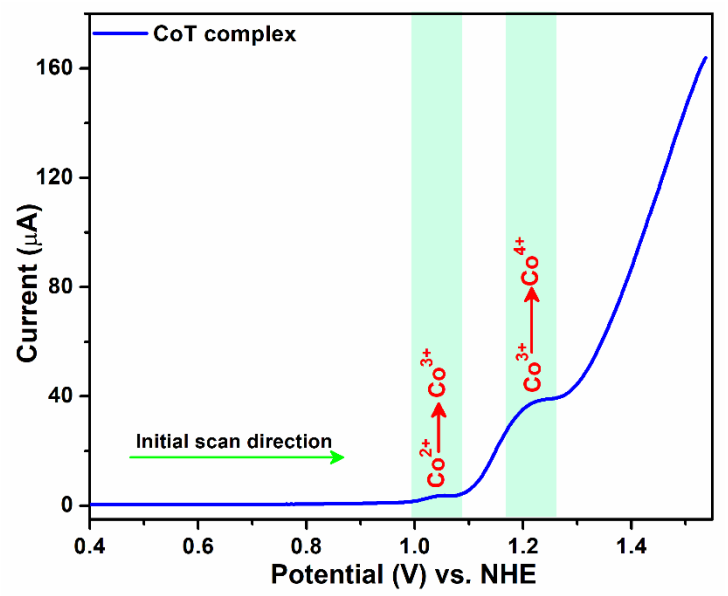

Fig. S33 Differential pulse voltammetry (DPV) plot of **CoT** complex.

==========

Section S4.2. Overpotential and Turnover frequency (TOF) of the electrodeposited CoO_x:

To compare the OER results of **CoT** complex with those of electrodeposited CoO_x, we have prepared an electrodeposited CoO_x material by performing the constant potential electrolysis of a 5 mM $CoCl_2 \cdot 6H_2O$ solution (in 0.1 M NaOAc electrolyte at pH 8.5) at a constant potential of 1.40 V (vs. NHE) over 2 h using glassy carbon as the working electrode, Ag/AgCl as a reference electrode, and Pt-wire as a counter electrode (Fig. S34, below). After this electrolysis, the GC electrode (used in CPE) is rinsed with water and placed into a fresh 0.1 M NaOAc electrolyte for CV measurement. In the obtained CV profile of the used GC electrode, the electrodeposited material (CoO_x) on the GC electrode shows a comparatively high catalytic current as compared with that shown by as-such $[Co(H_2O)_6]^{2+}$ (Fig. S35, below). Afterwards, we have performed several electrochemical experiments to calculate the overpotential and turnover frequency (TOF) values of this prepared electrodeposited CoO_x material, as described below.

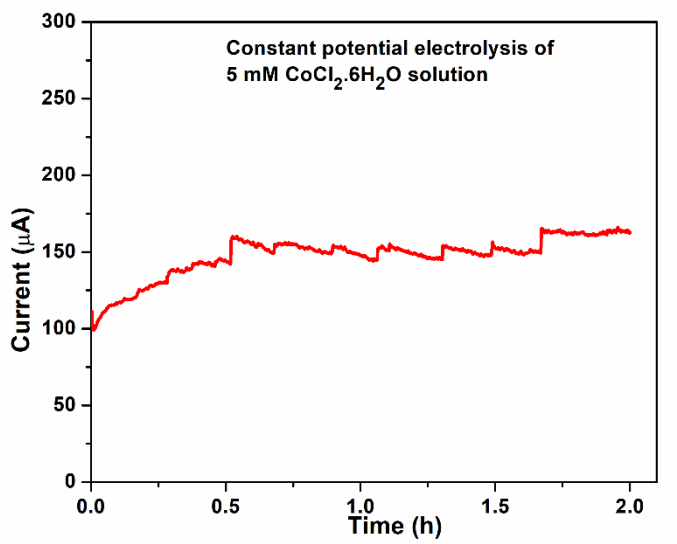

Fig. S34 Constant potential electrolysis of 5 mM $CoCl_2 \cdot 6H_2O$ solution at 1.40 V (vs. NHE) for 2 h using glassy carbon as the working electrode, Ag/AgCl as a reference electrode, and Pt-wire as a counter electrode, when electrodeposition of a coloured material occurs.

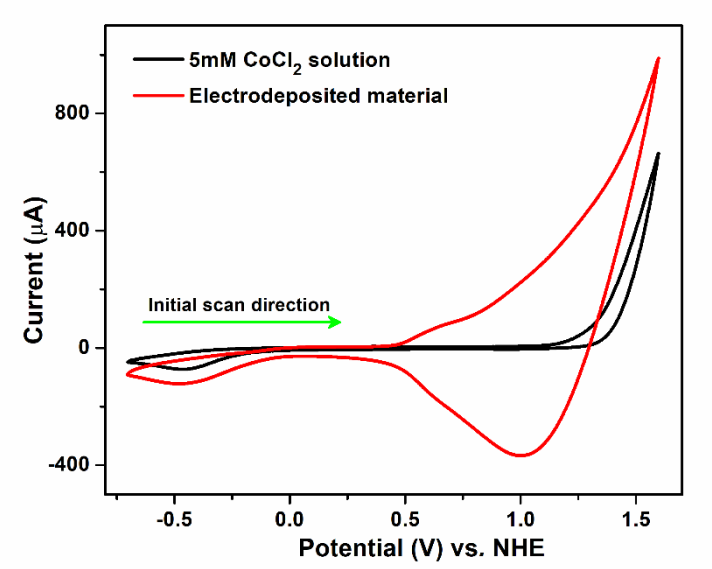

Fig. S35 CV diagrams of 5 mM $CoCl_2 \cdot 6H_2O$ solution (black line) and electrodeposited material on GC electrode in fresh 0.1 M NaOAc electrolyte (red line).

Overpotential:

After this electrolysis, the GC electrode (used in CPE) is rinsed with water and placed into a fresh 0.1 M NaOAc electrolyte for CV measurement. We have then calculated the overpotential and the turnover frequency value of the electrodeposited CoO_x material on the GC working electrode. To calculate the overpotential, a Tafel plot has been constructed, as shown in Fig. S36 (shown below). An overpotential of 282 mV is observed for electrodeposited CoO_x at a current density of 1 mA/cm^2 with a Tafel slope of 278 mV/decade.

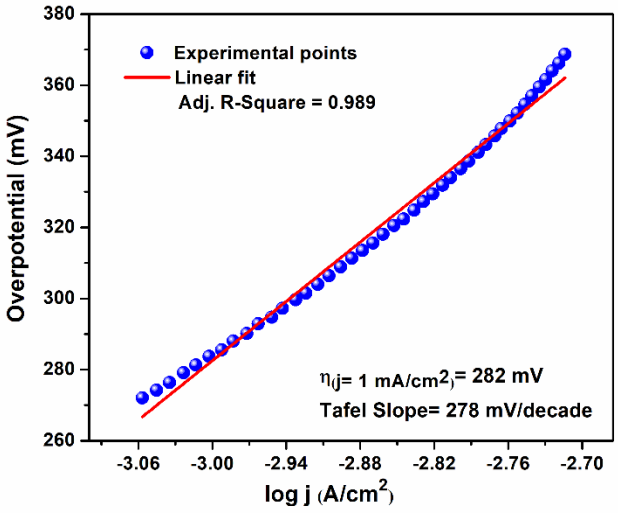

Fig. S36 Tafel plot of electrodeposited CoO_x on the GC working electrode.

Turnover frequency (TOF):

We have calculated the active Co atoms/cm^2 of the electrodeposited material (CoO_x) on the working electrode surface using a method recently described by Pintado et al.[4] by measuring the surface coverage (Γ_0) from the slope (1.12×10^{-3} F) of the peak current vs scan rate (Fig. S37) using the equation S4.

$$\text{Slope} = n^2F^2A\Gamma_0/4RT \qquad \text{(S4)}$$

Where 'n' = No. of electrons involved, here 2. For Co(III)/Co(II) and Co(IV)/Co(III) conversions.

'F' = 1 Farad = 96,500 C.

'A' = Geometrical surface area of electrode = 0.07 cm^2

'R' = Ideal Gas Constant = 8.314 J mol^{-1} K^{-1}

'T' = Temperature during experiment = 298 K

'Γ_0' = Surface density of active cobalt atoms.

Thus, the obtained surface density of active cobalt atoms (Γ_0) is 4.26×10^{-9} mol/cm^2.

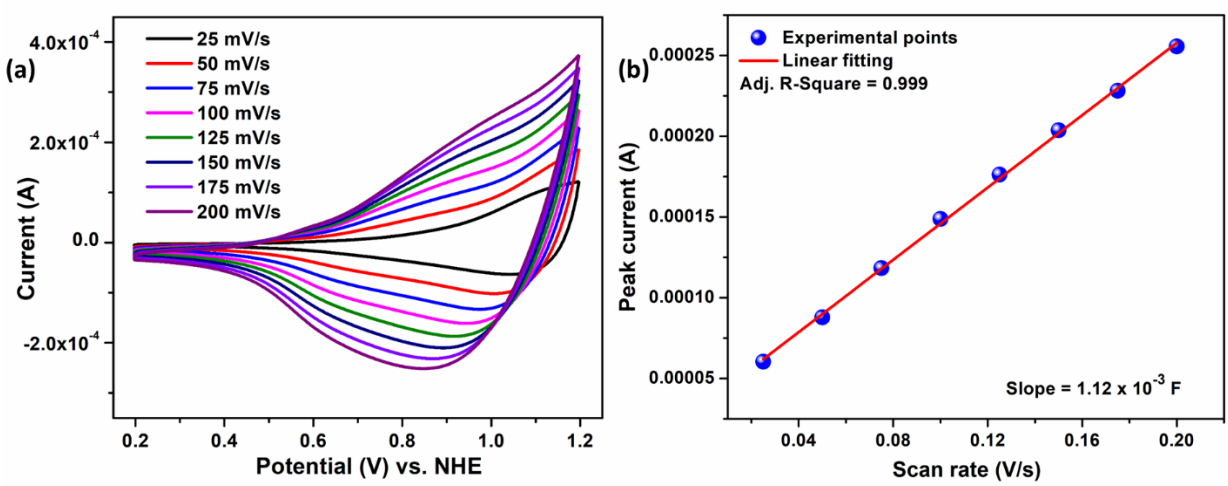

Fig. S37 (a) Scan rate variation of the electrodeposited CoO_x on the glassy carbon electrode; (b) peak current versus scan rate plot, obtained from Fig. S41a at a potential of 1.0 V (vs. NHE).

The activity of a catalyst can be well-expressed in terms of turnover frequency (TOF). It is defined as the number of reactant molecules converted into product molecules in unit time per active site. The TOF is measured using equations S5 and S6.

$$\text{TOF at overpotential of 282 mV} = \frac{Current\ density\ of\ 282\ mV\ overpotential}{4 \times F \times \Gamma 0} \quad \text{(S5)}$$

Or

$$\text{TOF at current density of 1 mA/cm}^2 = \frac{1\ mA/cm2}{4 \times F \times \Gamma 0} \quad \text{(S6)}$$

Thus, the TOF of the electrodeposited CoO_x is calculated as **0.61** s^{-1} at 282 mV overpotential at a pH value of 8.5.

==========

Table S2. Literature survey table comparing the electrocatalytic homogeneous OER kinetic parameters of various known cobalt-containing catalysts with those of the present work.

Compound	Electrolyte	Onset Overpotential (mV)	TOF (s^{-1})	Reference
$[Co^{II}(H_2O)(OAc)(Tris)_2]$ (**CoT**)	0.1 M NaOAc (pH 8.5)	461	0.51 h^{-1}	**This work**
$[Co^{III}(dpaq)(Cl)]Cl$	0.1 M phosphate	500	85	5

	buffer (pH 8.0)			
$CoH^{\beta F}CX–CO_2H$	0.1 M PBS (pH 7.0)	600	0.81	6
$[Co(TPA\text{-}R)]^{2+}$	0.1 M borate buffer (pH 8)	420	6.03	7
$[Co(Py5)(OH_2)](ClO_4)_2$	0.1 M phosphate buffer (pH 9.2)	500	79	8
$([TPA)_2Co_2\text{-}(\mu\text{-}OH)(\mu\text{-}O_2)](ClO_4)_3$	0.1 M borate buffer (pH 8)	540	1.4	9
$Na[(L^{4-})Co^{III}]$ L = substituted tetraamido macrocyclic ligand	0.1 M phosphate buffer (pH 7.0)	380	7.53	10
$[Co(bpbH_2)Cl_2]$	0.1 M of $[n\text{-}Bu_4N]ClO_4$ DMF (pH 8.6)	560	81.54	11
$Na_{10}[Co_4(H_2O)_2(PW_9O_{34})_2]$	0.1 M sodium phosphate buffer (pH 8)	578	0.98	12
UTSA-16 (MOF, Co4O4)	1 M KOH	408	-	13
UTSA-16 (MOF, Co4O4)	0.1 M KOH	500		
TPT_2Co	0.1 M phosphate buffer (pH 9)	350	108	14

References.

1. D. Jana, M. Todupunuri, M. Shavez and S. K. Das, Effective complexation of tris-ligand with $CoCl_2{\cdot}6H_2O$ in an aqueous solution: Suppressing electrochemical formation of CoO_x, *Inorg. Chem.*, 2025, **64**, 7841−7845.
2. S. Mukhopadhyay, J. Debgupta, C. Singh, A. Kar and S. K. Das, A keggin polyoxometalate shows water oxidation activity at neutral pH: POM@ZIF-8, an efficient and robust electrocatalyst, *Angew. Chem. Int. Ed.*, 2018, **130**, 1936 –1941.
3. S. Mukhopadhyay, O. Basu, A. Kar and S. K. Das, Efficient electrocatalytic water oxidation by Fe(salen)–MOF composite: Effect of modified microenvironment, *Inorg. Chem.*, 2020, **59**, 472−483.
4. S. Pintado, S. Goberna-Ferrón, E. C. Escudero-Adán and J. R. Galán-Mascarós, Fast and persistent electrocatalytic water oxidation by Co–Fe prussian blue coordination polymers, *J. Am. Chem. Soc.*, 2013, **135**, 13270-13273.
5. S. Biswas, S. Bose, J. Debgupta, P. Das and A. N. Biswas, Redox-active ligand assisted electrocatalytic water oxidation by a mononuclear cobalt complex, *Dalton Trans*., 2020, **49**, 7155–7165.

6. D. K. Dogutan, R. McGuire Jr. and D. G. Nocera, Electocatalytic water oxidation by Cobalt(III) Hangman β-Octafluoro corroles, *J. Am. Chem. Soc.*, 2011, **133**, 9178–9180.
7. S. Liu, Y. -J. Lei, Z. -J. Xin, R. -J. Xiang, S. Styring, A. Thapper and H. -Y. Wang, Ligand modification to stabilize the cobalt complexes for water oxidation, *Int. J. Hydrogen Energy,* 2017**, 40**, 29716-29724.
8. D. J. Wasylenko, C. Ganesamoorthy, J. B. Garcia and C. P. Berlinguette, Electrochemical evidence for catalytic water oxidation mediated by a high-valent cobalt complex, *Chem. Commun.*, 2011, **47**, 4249–4251.
9. H. -Y. Wang, E. Mijangos, S. Ott and A. Anders, Water oxidation catalyzed by a dinuclear cobalt–polypyridine complex, *Angew. Chem. Int. Ed.*, 2014, **53**, 14499 –14502.
10. H. -Y. Du, S. -C. Chen, X. -J. Su, L. Jiao and M. -T. Zhang, Redox-active ligand assisted multielectron catalysis: A case of Co^{III} complex as water oxidation catalyst, *J. Am. Chem. Soc.*, 2018, **140**, 1557−1565.
11. Z. -Q. Wang, L. -Z. Tang, Y. -X. Zhang, S. -Z. Zhan and J. -S. Ye, Electrochemical-driven water splitting catalyzed by a water-soluble cobalt(II) complex supported by N,N'-bis(2'-pyridinecarboxamide)- 1,2-benzene with high turnover frequency, *J. Power Sources*, 2015, **287**, 50-57.
12. J. J. Stracke and R. G. Finke, Water oxidation catalysis beginning with 2.5 μM $[Co_4(H_2O)_2(PW_9O_{34})_2]^{10-}$: Investigation of the true electrochemically driven catalyst at ≥600 mV overpotential at a glassy carbon electrode, *ACS Catal.*, 2013, **3**, 1209−1219.
13. J. Jiang, L. Huang, X. Liu and L. Ai, Bioinspired cobalt−citrate metal−organic framework as an efficient electrocatalyst for water oxidation, *ACS Appl. Mater. Interfaces*, 2017, **9**, 7193−7201.
14. G. Ruan, L. Engelberg, P. Ghosh and G. Maayan, A unique Co(III)-peptoid as a fast electrocatalyst for homogeneous water oxidation with low overpotential, *Chem. Commun.*, 2021, **57**, 939-942.

##########